AD-A257 176

NASA
Technical Memorandum 105718

AVSCOM
Technical Report 92–C–003

Minimization of Deviations of Gear Real Tooth Surfaces Determined by Coordinate Measurements

F.L. Litvin, C. Kuan, and J.-C. Wang
University of Illinois
Chicago, Illinois

R.F. Handschuh
Propulsion Directorate
U.S. Army Aviation Systems Command
Lewis Research Center
Cleveland, Ohio

J. Masseth
Dana Corporation
Fort Wayne, Indiana

and

N. Maruyama
Nissan Motor Corporation
1 Natsushima-cho, Yokosuka, Japan

Prepared for the
1992 Power Transmission and Gearing Conference
Phoenix, Arizona, September 13–16, 1992

DTIC
ELECTE
OCT 2 8 1992
S
A

NASA

US ARMY
AVIATION
SYSTEMS COMMAND

92-28316

MINIMIZATION OF DEVIATIONS OF GEAR REAL TOOTH SURFACES DETERMINED BY COORDINATE MEASUREMENTS

F. L. Litvin, C. Kuan and J.-C. Wang
(University of Illinois at Chicago)
R.F. Handschuh (NASA Lewis Research Center)
J. Masseth (the Dana Corporation)
N. Maruyama (the Nissan Motor Co.)

ABSTRACT

The deviations of a gear's real tooth surface from the theoretical surface are determined by coordinate measurements at the grid of the surface. A method has been developed to transform the deviations from Cartesian coordinates to those along the normal at the measurement locations. Equations are derived that relate the first order deviations with the adjustment to the manufacturing machine-tool settings. The deviations of the entire surface are minimized. The minimization is achieved by application of the least-square method for an overdetermined system of linear equations. The proposed method is illustrated with a numerical example for hypoid gear and pinion.

INTRODUCTION

Coordinate measurements of gear tooth surfaces coupled with the ability to correct the initially applied machine-tool settings is becoming a significant part of advanced gear technology. We may consider two stages of this technique:

(i) Application of coordinate measurements of the manufactured gears for numerical determination, in 3D space, of deviations of real tooth surfaces.

(ii) The goal of minimization of deviations can be achieved by proper corrections of initially applied machine-tool settings. The determination of corrected machine-tool settings is found numerically.

The technological aspects of the problem to-be discussed are as follows:

(i) The deviations of real tooth surfaces are inevitable due to surface distortion by heat-treatment, errors of initial machine-tool settings, deflection by manufacturing, etc.

(ii) Application of an additional finishing operation for elimination of the deviations would be too expensive in comparison with the approach based on corrections of initially applied machine-tool settings. The advantage of this approach is the possibility of using the same equipment to correct the deviations.

The disadvantage is that the approach will be successful only if the deviations are repeatable.

(iii) The coordinate measurements must be performed with high precision, which currently prohibits them from being performed simultaneously with the manufacturing. Therefore, the coordinate measurements are performed after manufacturing, but only the first gear of the whole gear set to-be manufactured is tested.

(iv) In some cases master-gears are used and the coordinate measurements provide the information about the deviations from the master-surface for the surface being tested. The authors consider this approach less effective as compared to computerized determination of surface deviations and corrections of machine-tool settings.

The mathematical solutions to this problem are represented in the Appendix to this paper. The technique described in the paper has been developed in the response to the increasing requirements of high quality gear transmissions. Minimizing the deviations of real tooth surfaces results in a reduction in the level of transmission errors that cause gear noise and vibration.

The proposed approach is applied to hypoid gear drives that have found a wide application in transmissions [1,2]. The contents of the paper are complemented with a numerical example for a hypoid pinion and gear to illustrate the effectiveness of the proposed approach. The level of deviations of the pinion surface has been reduced from 30 microns to the theoretical level of 2-3 microns.

1. OVERVIEW OF MEASUREMENT AND MODELLING METHOD

The approach developed in this paper enables the determination of deviations of a real surface from the known theoretical surface. This is accomplished by two steps: (i) coordinate measurements for determination of surface deviations and (ii) minimization of the deviations through correction of the previously applied machine-tool settings.

The surface deviations obtained initially in Cartesian coordinates are transformed into deviations along the normal to the theoretical surface. The coordinate measurements are performed by a machine with four or five degrees-of-freedom. In the case of four degrees-of-freedom, the probe performs three translational motions (fig. 1); the fourth motion, rotation, is performed by a rotary table. The axis of rotational motion coincides with the axis of the workpiece. In the case of a five degree-of-freedom machine, the fifth degree of freedom is used to provide the deflections of the probe in the direction of the normal to the theoretical surface. The probe is provided with a changeable spherical surface whose diameter can be chosen from a wide range.
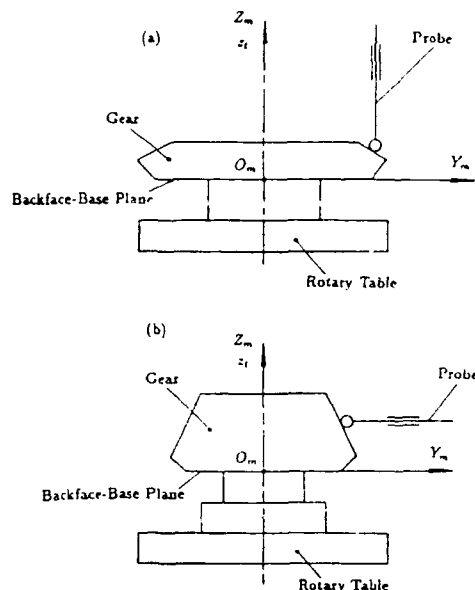

Fig. 1. Surface Measurement.

The motions of the probe and the workpiece by coordinate measurements are computer controlled and therefore a grid comprising of the set of surface points to be measured must be chosen (fig. 2). There is a *reference* point on the grid that is necessary for the initial installments of the probe. There are two orientations of the probe installment that are used to measure a gear (fig. 1(a)) and a pinion (fig. 1(b)), depending on the angle of the pitch cone.
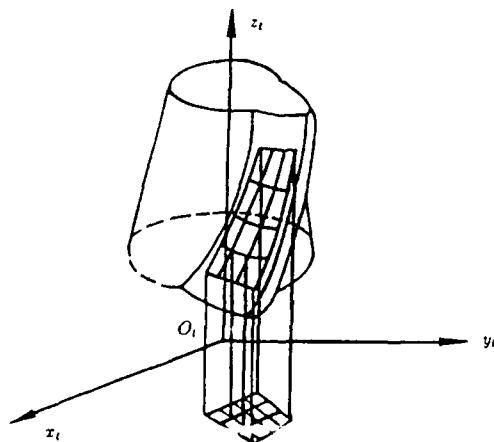

Fig. 2. Grid.

The mathematical aspects of coordinate measurements will now be described [2]: First, it is necessary to derive the equations of the theoretical surface. In many cases this surface can be derived as the envelope to the family of generating surfaces, namely the tool surfaces. Next, the results of coordinate measurements must be transformed into deviations of the real surface represented in the direction of the surface normal. Then, the relations between the surface variations and the corrections to the machine-tool settings must be determined. The surface deviations obtained from coordinate measurements and the surface variations determined by the corrections of machine-tool settings can be represented by an overdetermined system of linear equations. The number of these equations, k, is equal to the number of points of the grid, and the number of unknowns, m, is equal to the number of corrections of machine-tool settings ($m \ll k$). The optimal solution to such a system of linear equations results in the determination of the machine-tool setting corrections.

2. EQUATIONS OF THEORETICAL TOOTH SURFACE Σ_t

Considering that the theoretical surface can be determined directly, we represent it in coordinate system S_t in two parametric form as:

$$\mathbf{r}_t(u, \theta), \quad \mathbf{n}_t(u, \theta) \tag{1}$$

Here: $\mathbf{r}_t$ and $\mathbf{n}_t$ are the position-vector and the surface unit normal, respectively; (u, θ) are the Gaussian coordinates (surface coordinates).

For the case when surface Σ_t is the envelope to the family of generating surface Σ_c, we represent surface Σ_t and the unit normal $\mathbf{n}_t$ to Σ_t in S_t as [3]

$$\mathbf{r}_t = \mathbf{M}_{tc}\mathbf{r}_c(u_c, \theta_c), \quad f(u_c, \theta_c, \phi) = 0 \tag{2}$$

$$\mathbf{n}_t = \mathbf{L}_{tc}\mathbf{n}_c(u_c, \theta_c), \quad f(u_c, \theta_c, \phi) = 0 \tag{3}$$

Here: (u_c, θ_c) are the Gaussian coordinates of the generating surface Σ_c; ϕ is the generalized parameter of motion in the process for generation. The equation of meshing is given by:

$$f(u_c, \theta_c, \phi) = \mathbf{N}^{(c)} \cdot \mathbf{v}^{(ct)} = 0 \tag{4}$$

where $\mathbf{N}^{(c)}$ is the normal to Σ_c, $\mathbf{v}^{(ct)}$ is the relative motion for a point of contact of Σ_c and Σ_t. The 4×4 matrix $\mathbf{M}_{tc}$ and 3×3 matrix $\mathbf{L}_{tc}$ describe the coordinate transformation from S_c to S_t of a position vector and surface unit normal, respectively. Position vectors in 3-D space are represented with homogeneous coordinates.

3. COORDINATE SYSTEMS USED FOR COORDINATE MEASUREMENTS

Coordinate systems S_m and S_t are rigidly connected to the coordinate measuring machine (CMM) and the workpiece being measured, respectively (fig. 3). The back face of the gear is installed flush with the base plane of the CMM. The distance l between the origins O_m and O_t is known but the parameter of orientation δ must be determined (see section 4). The coordi-

nate transformation from S_t to S_m is represented by the matrix equation

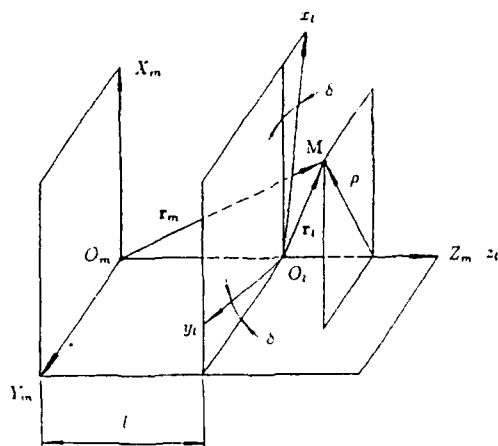$$\mathbf{r}_m = \mathbf{M}_{mt}\mathbf{r}_t \qquad (5)$$

Fig. 3. Coordinate Transformation.

4. GRID AND REFERENCE POINT

The grid is a set of points on Σ_t chosen as points of contact between the probe and Σ_t (fig. 3). Fixing the value of z_t for the point of the grid, and the value of, say y_t (or x_t), we can obtain the following equations

$$y_t(u_i, \theta_i) = h_i, \ z_t(u_i, \theta_i) = l_i \ (i = 1, \ldots, k) \qquad (6)$$

where k is the number of grid points.

We consider h_i and l_i as given and solve equations (6) for (u_i, θ_i). Then we can determine the position vectors and the unit normals for k points of the grid using the equations

$$\mathbf{r}_t^{(i)} = [x_t(u_i, \theta_i) \ y_t(u_i, \theta_i) \ z_t(u_i, \theta_i)]^T, \quad (i = 1, \ldots, k) \qquad (7)$$

$$\mathbf{n}_t^{(i)} = [n_{xt}(u_i, \theta_i) \ n_{yt}(u_i, \theta_i) \ n_{zt}(u_i, \theta_i)]^T, \quad (i = 1, \ldots, k) \qquad (8)$$

The position vector for the center of the probe, if the deviations are zero, is represented by the equation

$$\mathbf{R}_t^{(i)} = \mathbf{r}_t^{(i)} + \rho \mathbf{n}_t^{(i)} \quad (i = 1, \ldots, k) \qquad (9)$$

where ρ is the radius of the probe tip.

The reference point

$$\mathbf{r}_t^{(0)} = [x_t(u^{(0)}, \theta^{(0)}) \ y_t(u^{(0)}, \theta^{(0)}) \ z_t(u^{(0)}, \theta^{(0)})]^T \qquad (10)$$

is usually chosen as the mean point of the grid.

The center of the probe that corresponds the reference point on Σ_t is determined from equation (9) as

$$\mathbf{R}_t^{(0)} = [X_t(u^{(0)}, \theta^{(0)}) \ Y_t(u^{(0)}, \theta^{(0)}) \ Z_t(u^{(0)}, \theta^{(0)})]^T \qquad (11)$$

Here: $(u^{(0)}, \theta^{(0)})$ are known values.

The coordinates of the reference center of the probe are represented in coordinate system S_m of the measuring machine by the matrix equation

$$\mathbf{R}_m^{(0)} = \mathbf{M}_{mt}(\delta) \ \mathbf{R}_t^{(0)} \qquad (12)$$

Equation (12) yields

$$x_m^{(0)} = x_m^{(0)}(\delta, u^{(0)}, \theta^{(0)}) \\ y_m^{(0)} = y_m^{(0)}(\delta, u^{(0)}, \theta^{(0)}) \\ z_m^{(0)} = z_m^{(0)}(\delta, u^{(0)}, \theta^{(0)}) \qquad (13)$$

The three equations (13) contain four unknowns: δ, $x_m^{(0)}$, $y_m^{(0)}$, $z_m^{(0)}$. To solve these equations we may consider that one of the coordinates of the reference point of the probe center, say $y_m^{(0)}$, may be chosen equal to zero. Then the system of equations (13) allows the determination of δ, $x_m^{(0)}$ and $z_m^{(0)}$ [2]. Coordinates $x_m^{(0)}, y_m^{(0)} = 0, z_m^{(0)}$ are necessary for the initial installment of the center of the probe.

5. DEVIATIONS OF THE REAL SURFACE

The deviations of the real surface are caused by errors of manufacturing, heat treatment, etc. Vector positions of the center of the probe for the theoretical surface and the real surface can be represented as follow

$$\mathbf{R}_m = \mathbf{r}_m(u, \theta) + \rho \mathbf{n}_m(u, \theta) \qquad (14)$$

$$\mathbf{R}_m^* = \mathbf{r}_m(u, \theta) + \lambda \mathbf{n}_m(u, \theta) \qquad (15)$$

Here: $\mathbf{r}_m$ and $\mathbf{n}_m$ are the position vector and the unit normal to the theoretical surface, respectively, that are represented in coordinate system S_m of the measuring machine: λ determines the real location of the probe center and is considered along the normal to the theoretical surface; $\mathbf{R}_m$ and $\mathbf{R}_m^*$ represent in S_m the position vector of the probe center for the theoretical and real surfaces, respectively. Equations (14) and (15) yield

$$\mathbf{R}_m^* - \mathbf{R}_m = (\lambda - \rho)\mathbf{n}_m = \triangle n \mathbf{n}_m \qquad (16)$$

and

$$\triangle n = (\mathbf{R}_m^* - \mathbf{R}_m) \cdot \mathbf{n}_m \qquad (17)$$

The position vector $\mathbf{R}_m^*$ is determined by coordinate measurements for points of the grid. Equation (17) determines numerically the function:

$$\triangle n_i = \triangle n_i(u_i, \theta_i) \quad (i = 1, \ldots, k) \qquad (18)$$

that represents the deviations of the real surface for each point of the grid.

6. MINIMIZATION OF DEVIATIONS

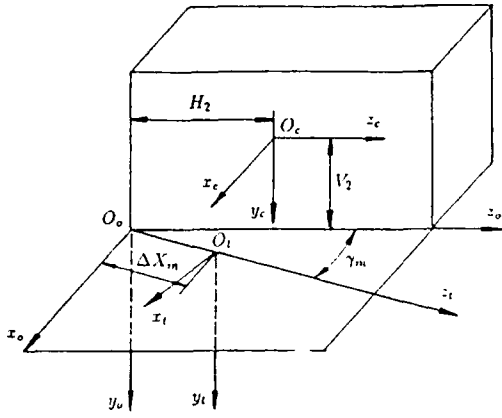The procedure of minimization of deviations can be repre-

sented in two stages: (i) determination of variations of theoretical surface caused by changes of applied machine-tool settings, and (ii) minimization of deviations of real surface by appropriate correction of machine-tool settings.

We consider that the theoretical surface is represented in S_t as

$$\mathbf{r}_t = \mathbf{r}_t(u, \theta, d_j) \quad (j = 1, \ldots, m) \tag{19}$$

where parameters d_j are the machine-tool settings.

The surface variations are represented by

$$\delta \mathbf{r}_t = \frac{\partial \mathbf{r}_t}{\partial u} \delta u + \frac{\partial \mathbf{r}_t}{\partial \theta} \delta \theta + \sum_{j=1}^{m} \frac{\partial \mathbf{r}_t}{\partial d_j} \delta d_j \tag{20}$$

We multiply both sides of equation (20) by the surface unit normal $\mathbf{n}_t$ and take into account that $\dfrac{\partial \mathbf{r}_t}{\partial \theta} \cdot \mathbf{n}_t = \dfrac{\partial \mathbf{r}_t}{\partial u} \cdot \mathbf{n}_t = 0$ since $\dfrac{\partial \mathbf{r}_t}{\partial \theta}$ and $\dfrac{\partial \mathbf{r}_t}{\partial u}$ lie in the plane that is tangent to the surface. Then we obtain:

$$\delta \mathbf{r}_t \cdot \mathbf{n}_t = (\sum_{j=1}^{m} \frac{\partial \mathbf{r}_t}{\partial d_j} \cdot \mathbf{n}_t) \delta d_j = \sum_{j=1}^{m} a \delta d_j \tag{21}$$

We can now consider a system of k linear equations in m unknowns ($m \ll k$) of the following structure

$$\left. \begin{array}{l} a_{11} \delta d_1 + a_{12} \delta d_2 + \ldots + a_{1m} \delta d_m = b_1 \\ \cdots\cdots\cdots\cdots\cdots\cdots\cdots\cdots\cdots\cdots\cdots\cdots\cdots\cdots\cdots \\ a_{k1} \delta d_1 + a_{k2} \delta d_2 + \ldots + a_{km} \delta d_m = b_k \end{array} \right\} \tag{22}$$

Here:

$$b_i = \triangle n_t = (\mathbf{R}_{mi}^* - \mathbf{R}_{mi}) \cdot \mathbf{n}_{mi} \tag{23}$$

where i designates the number of grid point; a_{sj} ($s = 1, \ldots, k$; $j = 1, \ldots, m$) represent the dot product of partial derivatives $\dfrac{\partial \mathbf{r}_t}{\partial d_j}$ and unit normal $\mathbf{n}_t$.

The system of linear equations (22) is overdetermined since $m \ll k$. The essence of the procedure of minimization of deviations is determination of such unknowns δd_j ($j = 1, \ldots, m$) that will minimize the difference between the left and right sides of equations (22). The solution was accomplished by the least-square method. The subroutine DLSQRR of IMSL MATH / LIBRARY [4] was used for computerization of the procedure.

The success of minimization of deviations depends on the number of parameters that may be varied (the number of machine-tool settings that may be corrected). The number of pinion machine-tool settings is larger than for the gear. The minimization of deviations can be performed for each pinion tooth side separately. However, it must be performed simultaneously for both sides of the gear tooth since the gear is cut by the duplex method. For these reasons the minimization of deviations for the pinion is more effective than for the gear (see below the numerical examples).

7. APPLICATION TO INSPECTION OF FORMATE HYPOID GEAR

Each tooth side of a formate face-milled gear is generated by

Fig. 4. Generating Cones for Format Face-milled Gear.

a cone and the gear tooth surface is the surface of the generating cone. Two cones that are shown in fig. 4(a) represent both sides of the gear space. The following equations represent in coordinate system S_c gear surfaces for both sides and the unit normals to such surfaces (fig. 4(b))

$$\mathbf{r}_c = \begin{bmatrix} -s_G \cos \alpha_G \\ (r_c - s_G \sin \alpha_G) \sin \theta_G \\ (r_c - s_G \sin \alpha_G) \cos \theta_G \\ 1 \end{bmatrix} \tag{24}$$

$$\mathbf{n}_c = \begin{bmatrix} \sin \alpha_G \\ -\cos \alpha_G \sin \theta_G \\ -\cos \alpha_G \cos \theta_G \end{bmatrix} \tag{25}$$

Here: $\mathbf{r}_c$ is the position vector and $\mathbf{n}_c$ is the surface unit normal; r_c is the cutter tip radius; α_G is the cutter blade angle ($\alpha_G > 0$ for the concave side and $\alpha_G < 0$ for the convex side).

Fig. 5 shows the installment of the generating cone on the cutting machine. Coordinate systems S_o and S_t are rigidly connected to the cutting machine and the gear being generated, respectively. Systems S_c, S_o and S_t are rigidly connected to each other since the gear is formate cut (no relative motion between the cutter and workpiece). To represent in S_t the theoretical gear tooth surface Σ_t and the unit normal to Σ_t we use the following matrix equations

$$\mathbf{r}_t(s_G, \theta_G, d_j) = \mathbf{M}_{tc} \, \mathbf{r}_c(s_G, \theta_G) \tag{26}$$

4

Fig. 5. Machine-tool Settings for Formate Face-milled Gear.

$$\mathbf{n}_t(s_G, \theta_G, d_j) = \mathbf{L}_{tc}\, \mathbf{n}_c(s_G, \theta_G) \tag{27}$$

where

$$\mathbf{M}_{tc} = \mathbf{M}_{to}\, \mathbf{M}_{oc}$$

$$= \begin{bmatrix} \cos\gamma_m & 0 & -\sin\gamma_m & 0 \\ 0 & 1 & 0 & 0 \\ \sin\gamma_m & 0 & \cos\gamma_m & -\Delta X_m \\ 0 & 0 & 0 & 1 \end{bmatrix} \begin{bmatrix} 1 & 0 & 0 & 0 \\ 0 & 1 & 0 & -V_2 \\ 0 & 0 & 1 & H_2 \\ 0 & 0 & 0 & 1 \end{bmatrix} \tag{28}$$

The surface Gaussian coordinates are s_G and θ_G and d_j (γ_m, V_2, H_2 and ΔX_m) are the machine-tool settings.

The numerical example presented in this paper is based on the experiment that has been performed at the Dana Corporation (Fort Wayne, USA). The initial deviations Δn for each side of real tooth surface have been obtained by measurements on a coordinate measuring machine (fig. 1). The grid for the measurements is formed by nine sections along the tooth length with each section having five points. The number k of grid points is therefore 45 and the reference point is at the middle of the grid, (i.e., the third point of the fifth section). In the measurement, the coordinate $y_m^{(0)}$ of the reference point is chosen to be zero and the alignment angle δ is determined from solving equation system (13).

The minimization of deviations was performed in accordance to the algorithm described in section 6 for the formate cut gear. The measurement of the initial and final deviations are shown in figures 6-8. The machine-tool settings initially used and corrected are shown in Table 1.

7. EQUATIONS OF PINION THEORETICAL TOOTH SURFACE

The pinion tooth surface is generated as the envelope to the family of tool surfaces that are cone surfaces (fig. 9).

Henceforth, we will consider the following coordinate systems:
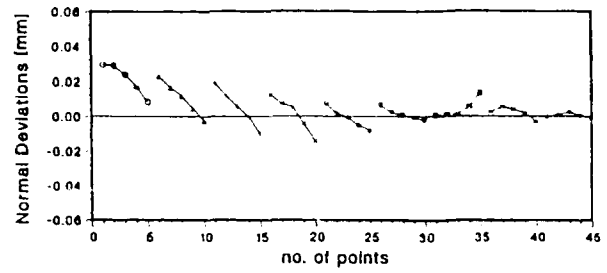
Fig. 6. Deviations of Gear Real Tooth Surface (Driving Side).
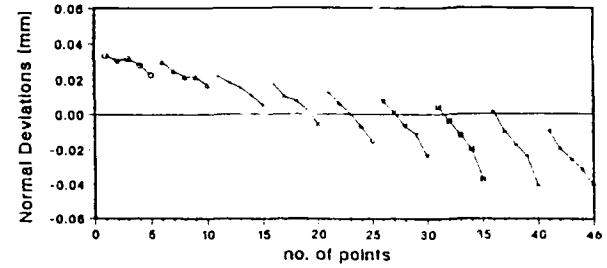
Fig. 7. Deviations of Gear Real Tooth Surface (Coast Side).
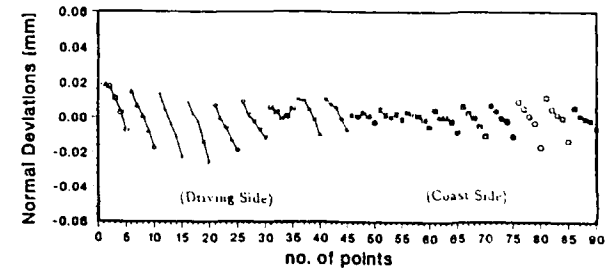
Fig. 8. Minimized Deviations of the Gear.

Table 1: Results of Gear Minimization

Machine Setting	Initial	Corrected
Pressure Angle α_G	21.25°	21.25°
Cutter Diameter, mm (in)	228.6 (9)	228.6 (9)
Point Width of Cutter, mm (in)	2.03 (.08)	2.03 (.08)
V_2, mm (in)	103.252550 (4.06506)	103.25220 (4.06505)
H_2, mm (in)	27.4666 (1.08136)	27.21603 (1.07150)
γ_m, rad.	1.059816	1.06437
ΔX_m, mm (in)	0.009677 (.00038)	-0.53343 (-0.0210)

(i) the fixed ones, S_0 (x_0, y_0, z_0) and S_q (x_q, y_q, z_q) that are rigidly connected to the cutting machine (fig. 10 and fig. 11); (ii) the movable coordinate systems S_c and S_p that are rigidly connected to the cradle of cutting machine and the pinion, respectively; (iii) coordinate system S_t that is rigidly connected to the head cutter. In the process of generation the cradle with S_c performs rotational motion about the z_o-axis with angular velocity $\omega^{(c)}$, and the pinion with S_p performs rotational motion about the x_q-axis with angular velocity $\omega^{(p)}$ (fig. 11).

The tool (head-cutter) is mounted on the cradle and performs rotational motion with the cradle. Coordinate system S_t is rigidly connected to the cradle. To describe the installment of the tool
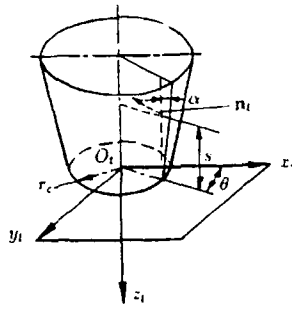
(a) Head-Cutter Surface Parameters
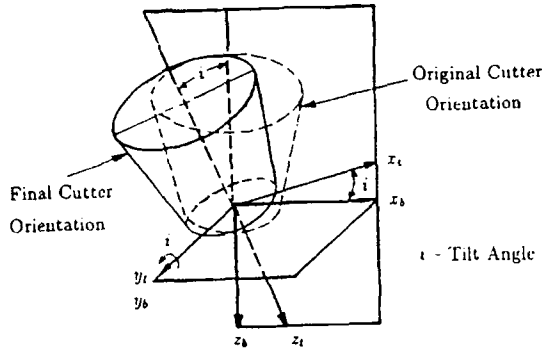
(b) Coordinate Systems for Head-Cutter Tilt

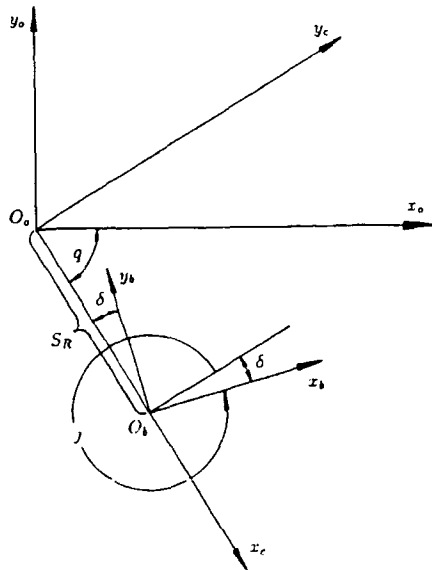Fig. 9. Pinion Head-cutter Surface.

Fig. 10. Cutting Machine and Cradle Coordinate Systems.

with respect to the cradle we use coordinate system S_b (fig. 9 and fig. 10). The required orientation of the head-cutter with respect to the cradle is accomplished as follows: (i) coordinate systems S_b and S_t are rigidly connected and then they are turned as one rigid body about the z_c-axis through the swivel angle $j = 2\pi - \delta$ (fig. 10); (ii) then the head-cutter with coordinate system S_t is tilted about the y_b-axis under the angle i (fig. 9(b)). The head-cutter is rotated about its axis z_t but the angular velocity in this
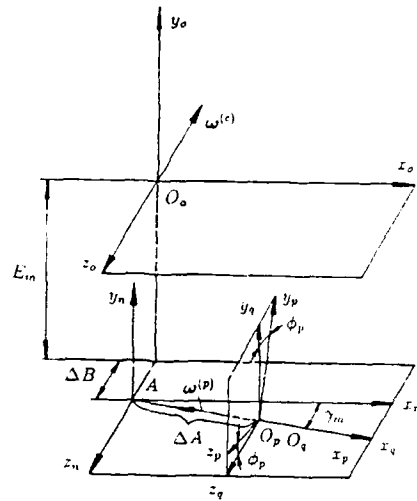
Fig. 11. Angular Velocities of Cradle and Pinion.

motion is not related with the generation process and depends only on the desired velocity of cutting.

It will be shown later that the deviations of real pinion tooth surface can be minimized by corrections of parameters of install-ment of the pinion and the head-cutter. These pinion setting parameters are E_m — the machine offset, γ_m — the machine-root angle, ΔB — the sliding base, ΔA — the machine center to back (fig. 11). The head-cutter settings parameters are: S_R — radial setting, θ_c — initial value of cradle angle, j — the swivel angle (fig. 10) , and i — the tilt angle (fig. 9(b)).

Tool Surface Equations

The head-cutter surface is a cone and is represented in S_t (fig. 9) as

$$\mathbf{r}_t(s,\theta) = \begin{bmatrix} (r_c + s \sin \alpha) \cos \theta \\ (r_c + s \sin \alpha) \sin \theta \\ -s \cos \alpha \\ 1 \end{bmatrix} \quad (29)$$

Here: (s, θ) are the Gaussian coordinates, α is the blade angle and r_c is the cutter point radius. Vector function (29) with α positive and α negative represents surfaces of two head-cutters that are used to cut the pinion concave side and convex side, respectively.

The unit normal to the head-cutter surface is represented in S_t by the equations

$$\mathbf{n}_t = [-\cos \alpha \cos \theta \quad -\cos \alpha \sin \theta \quad -\sin \alpha]^T \quad (30)$$

The Family of Tool Surfaces is represented in S_p by the matrix equation

$$\mathbf{r}_p(s, \theta, \phi_p) = \mathbf{M}_{pq} \mathbf{M}_{qn} \mathbf{M}_{no} \mathbf{M}_{oc} \mathbf{M}_{cb} \mathbf{M}_{bt} \mathbf{r}_t(s, \theta) \quad (31)$$

Here: S_n is an auxiliary fixed coordinate system whose axes parallel to S_o axes.

6

$$\mathbf{M}_{bt} = \begin{bmatrix} \cos i & 0 & \sin i & 0 \\ 0 & 1 & 0 & 0 \\ -\sin i & 0 & \cos i & 0 \\ 0 & 0 & 0 & 1 \end{bmatrix}$$

$$\mathbf{M}_{cb} = \begin{bmatrix} -\sin j & -\cos j & 0 & S_R \\ \cos j & -\sin j & 0 & 0 \\ 0 & 0 & 1 & 0 \\ 0 & 0 & 0 & 1 \end{bmatrix}$$

$$\mathbf{M}_{oc} = \begin{bmatrix} \cos q & \sin q & 0 & 0 \\ -\sin q & \cos q & 0 & 0 \\ 0 & 0 & 1 & 0 \\ 0 & 0 & 0 & 1 \end{bmatrix}$$

$$\mathbf{M}_{no} = \begin{bmatrix} 1 & 0 & 0 & 0 \\ 0 & 1 & 0 & E_m \\ 0 & 0 & 1 & -\triangle B \\ 0 & 0 & 0 & 1 \end{bmatrix}$$

$$\mathbf{M}_{qn} = \begin{bmatrix} \cos\gamma_m & 0 & \sin\gamma_m & -\triangle A \\ 0 & 1 & 0 & 0 \\ -\sin\gamma_m & 0 & \cos\gamma_m & 0 \\ 0 & 0 & 0 & 1 \end{bmatrix}$$

$$\mathbf{M}_{pq} = \begin{bmatrix} 1 & 0 & 0 & 0 \\ 0 & \cos\phi_p & \sin\phi_p & 0 \\ 0 & -\sin\phi_p & \cos\phi_p & 0 \\ 0 & 0 & 0 & 1 \end{bmatrix}$$

$\delta = 2\pi - j$; $q = \theta_c + m_{cp}\phi_p$ where θ_c is the initial cradle angle and $m_{cp} = \omega^{(c)}/\omega^{(p)}$.

Equation of Meshing

This equation is represented as [3]:

$$\mathbf{n}^{(p)} \cdot \mathbf{v}^{(cp)} = \mathbf{N}^{(p)} \cdot \mathbf{v}^{(cp)} = f(s, \theta, \phi_p) = 0 \qquad (32)$$

where $\mathbf{n}^{(p)}$ and $\mathbf{N}^{(p)}$ are the unit normal and the normal to the tool surface, and $\mathbf{v}^{(cp)}$ is the velocity in relative motion.

Equation (32) is invariant with respect to the coordinate system where the vectors of the scalar product are represented. These vectors in our derivations have been represented in S_o as follows,

$$\mathbf{n}_o = \mathbf{L}_{oc}\,\mathbf{L}_{cb}\,\mathbf{L}_{bt}\,\mathbf{n}_t$$

$$\mathbf{v}_o^{(cp)} = [(\,\omega_o^{(c)} - \omega_o^{(p)}) \times \mathbf{r}_o] + (\overline{O_oA} \times \omega_o^{(p)})$$

Here:

$$\mathbf{r}_o = \mathbf{M}_{oc}\,\mathbf{M}_{cb}\,\mathbf{M}_{bt}\,\mathbf{r}_t$$

$$\overline{O_oA} = \begin{bmatrix} 0 & -E_m & \triangle B \end{bmatrix}^T$$

$$\omega_o^{(p)} = -\begin{bmatrix} \cos\gamma & 0 & \sin\gamma \end{bmatrix}^T \;;\; (|\,\omega_o^{(p)}| = 1)$$

$$\omega_o^{(c)} = -\begin{bmatrix} 0 & 0 & m_{cp} \end{bmatrix}^T$$

Pinion Tooth Surface

Equations (31) and (32) represent the pinion tooth surface in three-parametric form with parameters s, θ and ϕ_p. However, since equation (32) is linear with respect to s we can eliminate s and represent the pinion tooth surface in two-parametric form as

$$\mathbf{r}_p(\theta, \phi_p, d_j) \qquad (33)$$

Here: d_j $(j = 1, \ldots, 8)$ designate the installment parameters: $E_m, \gamma_m, \triangle B, \triangle A, S_R, \theta_c, j$ and i.

The normal to the pinion tooth surface is represented as

$$\mathbf{n}_p(\theta, \phi_p, d_k) \qquad (34)$$

where d_k $(k = 1, 2, 3, 4)$ designate the installment parameters γ_m, θ_c, j and i.

Results of Minimization

Fig. 12 and fig. 13 illustrate the initial deviations $\triangle b_i$ of the real surface, that have been obtained by measurements and calculations for the concave side and convex side, respectively. The blank data, the basic machine-tools settings, the corrections of machine-tool settings and the corrected machine-tool settings are shown in Table 2-3. Based on the corrected machine-tool settings, we can manufacture a new surface that will optimally fit the theoretical surface after the surface is distorted by manufacturing processes and heat treatment. The minimized deviations between the new surface and the theoretical surface are shown in fig. 14 and fig. 15. These figures confirm the effectiveness of the proposed approach. The deviations of approximately 30 microns have been reduced to 2-3 microns.

8. CONCLUSION

A general approach for computerized determination of deviations of a real surface from the theoretical one based on coordinate measurements has been proposed. An algorithm for minimization of deviations by corrections of initially applied machine-tool settings through application of a least square approach has been developed. The approach is illustrated with an example of the tooth surface of a hypoid pinion and gear.

REFERENCES

1. Gleason Works, 1987, "G-Age T.M. User's Manual ", for the Gleason Automated Gear Evaluation System Used with Zeiss Coordinate Measuring Machines.

2. Litvin, F.L., Zhang, Y., Kieffer, J., Handschuh, R. F., "Identification and Minimization of Deviations of Real Gear Tooth Surfaces", ASME Journal of Mechanical Design, Mar. 1991, pp. 55-62.

3. Litvin, F. L., 1989, "Theory of Gearing", NASA publications; RP-1212 (AVSCOM technical report; 88-c-035).

4. Dongarra, J. J., Bunch, J. R., Moler, C. B., and Stewart, G. W., 1979, "LINPACK User's Guide", SIAM, Philadelphia.

5. Litvin, F. L., Zhang, Y., Kuan, C., and Handschuh, R. F., "Computerized Inspection of Real Surfaces and Minimization of their Deviations", Proceedings of International Conference on Metrology and Properties of Engineering Surfaces, England, 10th -12th, April 1991.

Table 2: Blank Data of Hypoid Pinion

Number of Teeth = 13
Shaft Angle = 1.57079 rad.
Pitch Diameter = 88.22 mm
Outside Diameter = 103.96 mm
Pitch Angle = 0.32055 rad.
Face Angle = 0.41480 rad.
Root Angle = 0.30136 rad.
Mean Spiral Angle = 0.84677 rad.
Face Width = 38.30 mm
Whole Width = 11.63 mm
Hand of Spiral : R. H.
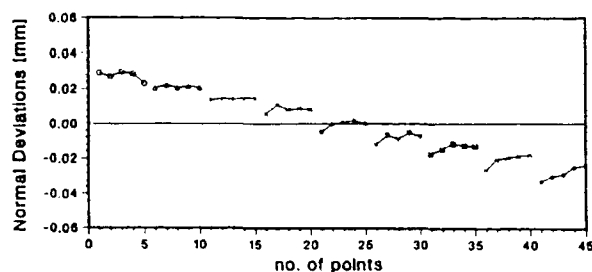
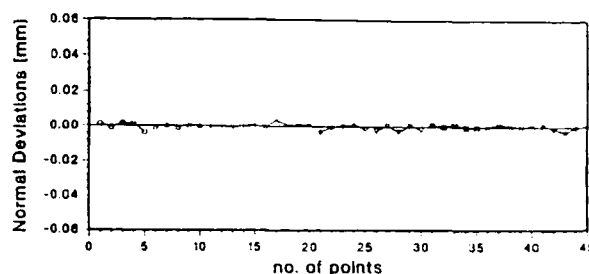Fig. 12. Deviations of Pinion Real Tooth Surface (Concave Side).

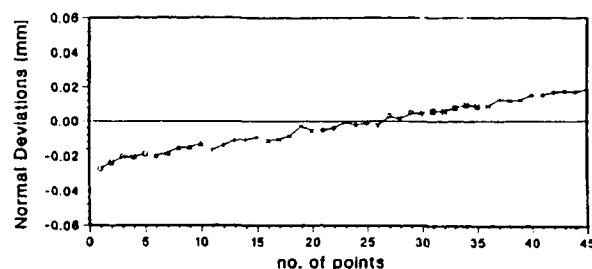Fig. 14. Minimized Deviations of the Pinion (Concave Side)

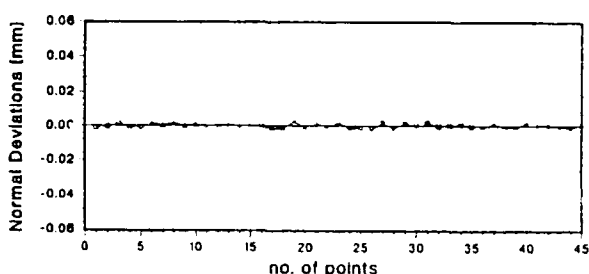Fig. 13. Deviations of Pinion Real Tooth Surface (Convex Side).

Fig. 15. Minimized Deviations of the Pinion (Convex Side)

Table 3: Basic, Corrected, and Machine-Tool Setting Differences of the Pinion
(Unit: Length in mm; Angle in rad.)

Machine Setting	Basic Machine-Tool Settings		Corrected Machine-Tool Settings		Setting Differences	
	Convex Side	Concave Side	Convex Side	Concave Side	Convex Side	Concave Side
Basic Tilt Angle	0.3761899	0.4104054	0.3712125	0.4360375	-0.4977365E-02	0.2563208E-01
Swivel Angle	5.766247	6.000656	5.768892	6.042021	0.2644968E-02	0.4136530E-01
Machine Root Angle	6.233736	6.229372	6.236861	6.202894	0.3125239E-02	-0.2647799E-01
Cradle Angle	4.846199	1.566173	4.845308	1.573228	-0.8908187E-03	0.7054806E-02
Radial Setting	114.0236	109.6660	113.6455	110.4463	-0.3780939	0.7803197
Sliding Base	23.87000	14.82000	23.87000	14.82000	0.0000000E+00	0.0000000E+00
Machine Center to Back	3.280000	-3.100000	3.767510	-3.970493	0.5769074E-01	-0.5540259
Blank Offset	-40.12000	-34.58000	-39.63248	-35.45049	0.4875103	-0.8701921
Cutting Ratio	0.3020446	0.3230215	0.3020446	0.3230215	0.0000000E+00	0.0000000E+00
Cutter Point Radius	114.9350	113.0300	114.9350	113.0300	0.0000000E+00	0.0000000E+00
Cutter Blade Angle	-0.5410521	0.2443461	-0.5410521	0.2443461	0.0000000E+00	0.0000000E+00

REPORT DOCUMENTATION PAGE

Public reporting burden for this collection of information is estimated to average 1 hour per response, including the time for reviewing instructions, searching existing data sources, gathering and maintaining the data needed, and completing and reviewing the collection of information. Send comments regarding this burden estimate or any other aspect of this collection of information, including suggestions for reducing this burden, to Washington Headquarters Services, Directorate for Information Operations and Reports, 1215 Jefferson Davis Highway, Suite 1204, Arlington, VA 22202-4302, and to the Office of Management and Budget, Paperwork Reduction Project (0704-0188), Washington, DC 20503

1. AGENCY USE ONLY (Leave blank)	2. REPORT DATE September 1992	3. REPORT TYPE AND DATES COVERED Technical Memorandum

4. TITLE AND SUBTITLE

Minimization of Deviations of Gear Real Tooth Surfaces Determined
by Coordinate Measurements

5. FUNDING NUMBERS

WU-505-63-36
1L162211A47A

6. AUTHOR(S)

F.L. Litvin, C. Kuan, J.-C. Wang, R.F. Handschuh,
J. Masseth, and N. Maruyama

7. PERFORMING ORGANIZATION NAME(S) AND ADDRESS(ES)

NASA Lewis Research Center
Cleveland, Ohio 44135-3191
and
Propulsion Directorate
U.S. Army Aviation Systems Command
Cleveland, Ohio 44135-3191

8. PERFORMING ORGANIZATION REPORT NUMBER

E-7115

9. SPONSORING/MONITORING AGENCY NAMES(S) AND ADDRESS(ES)

National Aeronautics and Space Administration
Washington, D.C. 20546-0001
and
U.S. Army Aviation Systems Command
St. Louis, Mo 63120-1798

10. SPONSORING/MONITORING AGENCY REPORT NUMBER

NASA TM-105718
AVSCOM TR-92-C-003

12a. DISTRIBUTION/AVAILABILITY STATEMENT

Unclassified - Unlimited
Subject Category 37

12b. DISTRIBUTION CODE

13. ABSTRACT (Maximum 200 words)

The deviations of a gear's real tooth surface from the theoretical surface are determined by coordinate measurements
at the grid of the surface. A method has been developed to transform the deviations from Cartesian coordinates to
those along the normal at the measurement locations. Equations are derived that relate the first order deviations with
the adjustment to the manufacturing machine-tool settings. The deviations of the entire surface are minimized. The
minimization is achieved by application of the least-square method for an overdetermined system of linear equations.
The proposed method is illustrated with a numerical example for hypoid gear and pinion.

14. SUBJECT TERMS

Gear; Grid surface; Deviations of gear; Measurements

15. NUMBER OF PAGES 10

16. PRICE CODE A02

17. SECURITY CLASSIFICATION OF REPORT	18. SECURITY CLASSIFICATION OF THIS PAGE	19. SECURITY CLASSIFICATION OF ABSTRACT	20. LIMITATION OF ABSTRACT
Unclassified	Unclassified	Unclassified	